The origin of the Redshift Spikes in the reflection spectrum of a Few-cycle Pulse in a Dense Medium

Yue-Yue Chen,[1] Xun-Li Feng,[2] Zhi-Zhan Xu,[1] and Chengpu Liu[1, *]

[1]State Key Laboratory of High Field Laser Physics,
Shanghai Institution of Optics and Fine Mechanics,
Chinese Academy of Sciences, Shanghai 201800, China
[2]Department of Physics, Shanghai Normal University, Shanghai 200234, China

We give a detailed description about the reflected spectrum of a few-cycle pulse propagating through a resonant dense medium. An unexpected low-frequency spike appeared in the red edge of the spectrum. To figure out the origin of this redshift spike, we analysis the mechanisms responsible for the redshift of the reflected field. So far, the redshift has not been well studied for few-cycle pulses except a brief explanation made by the previous study [Kaloshan *et al.*, Phys. Rev. Lett. 83 544 (1999).], which attributed the origin of the redshift to the so-called intrapulse four-wave mixing. However, we demonstrate numerically that the redshift consists of two separated spikes is actually produced by the Doppler effect of backpropagation waves, which is an analogue effect of dynamic nonlinear optical skin effect. Our study elucidates the underlying physics of the dynamic nonlinear optical effects responsible for the redshift spikes. Moreover, the dependency of the their frequency on the laser and medium parameters, such as medium density and input pulse area are also discussed.

PACS numbers: 42.65.Re, 42.50.Gy

With the rapid development of ultrafast science technology [1, 2], the field of optics soon entered the new era of extreme nonlinear optics. The interaction between a few cycles pulse with less than 5fs duration and resonant two-level system gives rise to a wealth variety of new phenomena, effects and applications. In this regime, the standard approximations used in the traditional nonlinear optics are no longer appropriate [3]. In this case, the full Maxwell-Bloch (MB) equations without slowly varying envelop approximation (SVEA) and rotating wave approximation (RWA) need to be solved, which can be done by an iterative predictor-corrector finite-difference time-domain method. Backpropagation is result from the self-reflection occurred in a saturable medium. The ability to solve the full Maxwell equation numerically fuels the study on the backpropagation of pulse ignored in the "one-way going" approximation [4] which is implied in envelope forms of MB equation. However, for a dense medium, backpropagation may has a significant impact on both the reflected and transmitted field, and a vast variety of intriguing new physical phenomena are emerged such as dynamic nonlinear optical skin (DNOS) effect [5] and decay of self-induced-transparency pulses [6].

The reflection spectrum of the few-cycle pulses has many unique features, and the most conspicuous one is the redshift observed in [7]. We also notice that, at the redside of the spectrum, an unexpected low-frequency spike is located at the red edge, along with another peak with higher frequency. To tell the mechanism behind those redspikes, we resort to the existing few-cycle theo-

ries about the physical interpretation of the observed redshift given by [7, 8], where the redshift is briefly attribute to intrapulse third-order four-wave mixing(FWM). However, the obtained scaling laws in terms of laser or medium parameters are inconsistent with FWM theory in so many ways. On the contrary, both the reflected field profile and spectrum can be explained very well with the Doppler effect of the backpropagation. This theory is based on the fact that the self-reflect interface is propagating through the medium with the transmitted pulse, which acts as a moving mirror inducing a redshift in the backpropagation waves [5].

In this letter, we fully study the mechanism of the redshift observed in the reflection spectrum of a few-cycle pulse propagating through a dense two-level atomic medium (DTLA). Our study is focused on the redshift spikes observed in the reflection spectrum and make clear the underlying physics by a theory based on the doppler effect of moving self-reflection interface instead of FWM. For the redspike with the largest shift, we also show how to change its location and amplitude by varying laser or medium parameters.

Assume the electromagnetic field is linearly polarized $E = E_x(z), H = H_y(z)$. The spatial orientation of the dipole is along x, and the macroscopic nonlinear polarization $P = P_x(z)$. The Maxwell equations for the DTLA medium takes the form [9]

$$\partial_t H_y = -\frac{1}{\mu_0}\partial_z E_x, \qquad (1)$$
$$\partial_t E_x = -\frac{1}{\epsilon_0}\partial_z H_y - \frac{1}{\epsilon_0}\partial_t P_x.$$

The off-diagonal density matrix element $\rho_{12} = (u+iv)/2$, and the population inversion $w = \rho_{22} - \rho_{11}$ between ex-
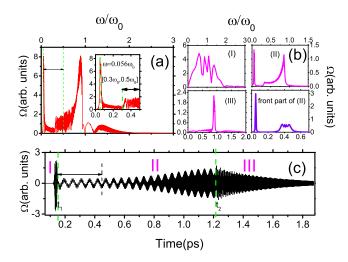
FIG. 1: Electric field profile and spectrum for three successional time regions. $\omega_c = 0.1\text{fs}^{-1}$, $A = 4\pi$, $L = 150\mu\text{m}$, $t_1 = 0.15\text{ps}$, $t_2 = 1.21\text{ps}$. $[t_i, t_1]$, $[t_1, t_2]$ and $[t_2, t_f]$ are labeled by I,II and III respectively. The below insets are the corresponding spectrums for those three regions, while the above inset is the spectrum of the first five oscillations in region II.

cited and ground state. u, v and w obey the following set of Bloch equations,

$$\begin{aligned}
\partial_t u &= -\gamma_2 u - \omega_0 v, \\
\partial_t v &= -\gamma_2 u + \omega_0 v + 2\Omega w, \qquad (2) \\
\partial_t w &= -\gamma_1 (w - w_0) - 2\Omega v.
\end{aligned}$$

Where γ_1, γ_2 are, respectively, the population and polarization relaxation constants, ω_0 is the resonant frequency, $\Omega(\Omega = dE_x/\hbar)$ is Rabi frequency, and w_0 is the initial population difference. The MB equation can be solved by adopting Yee's finite-difference time-domain discretization method for the electromagnetic fields and the predictor-corrector method for the medium variables [10–13]. The initial condition for the input pulse is $\Omega(t = 0, z) = \Omega_0 \cos[\omega_p(z-z_0)/c] \sec h[1.76(z-z_0)/(c\tau_p)]$, where Ω_0 is the peak Rabi frequency for the input pulse, τ_p is the full width at half maximum (FWHM) of the pulse intensity envelop, and the initial position z_0 is set to be a value large enough to avoid the pulse penetrating into the medium at $t = 0$. The medium is initialized with $u = v = 0, w_0 = -1$. To study the reflection of the pulse, we adopt the following parameters to integrate MB equation: $\omega_0 = \omega_p = 2.3\text{fs}^{-1}$, $z_{in} = 52.5\mu\text{m}, z_{out} = 202.5\mu\text{m}, z_0 = 26.25\mu\text{m}, d = 2\times10^{29}\text{Asm}$, $\gamma_1^{-1} = 1\text{ps}, \gamma_2^{-1} = 0.5\text{ps}, \tau_p = 5\text{fs}, \Omega_0 = 1.408\text{fs}^{-1}$,the corresponding pulse area $A(z) = d/\hbar \int_{-\infty}^{\infty} E_0(z, t')dt' = \Omega_0\tau_p\pi/1.76 = 4\pi$. Define a collective frequency parameter $\omega_c = Nd^2/\epsilon_0\hbar = 0.1\text{fs}^{-1}$ to represent the coupling strength between medium and field.

With the above parameters, we obtain the reflection spectrum as shown in Fig.1(a). It can be seen, the spectrum is generally composed of two red peaks, a sharp low-frequency spike and a broader one with higher frequency. Here we denote this two spikes as redspike I and II. The unexpected redspike I appears in the red edge centered at $\omega = 0.056\omega_0$ with a FWHM $\tau = 0.01\omega_0$ as shown in the inset of Fig.1(a). While the other has a wider frequency ranging from $0.3\omega_0$ to ω_0. To figure out the origin of these redspikes, we divide the reflected pulse into three successional time regions according to the electric profiles, as shown in Fig.1 (c). The first three pictures in Fig.1 (b) show the corresponding spectrums of the three regions and last one is the spectrum of the fist five waves in region II. It can be seen both redspike I and II appear in spectrum II, which are corresponding to a low-frequency modulation and a time-dependent frequency generated during the propagation in region II, respectively. In the following text, we analysis the underlying physics behind the electric profile in each region to reveal the origin of these redspikes.

In region I, when a few-cycle pulse propagates along +z in vacuum to a surface of a spatially homogeneous DTLA materials, an absorption front is built near the surface, which separates the excited and ground state, as shown in Fig.2(a). If the induced nonlinear polarization is sufficiently large, which can be achieved by raising density, to result in spatial inhomogeneities $n(\omega) \to n(\omega, z)$ rapidly, a wave propagating along -z may arise because of the constructive interference of reflections from individual spatial inhomogeneities [6]. Fig.2 (c) depicts the profile of the reflected field in region I, a ringing appears owing to the interference between the incident and the backpropagation waves. From the corresponding spectrum illustrated in Fig.2 (e), we can see that a remarkable redshift is observed in the spectrum with considerable spectral broadening and modulation compared with the input spectrum. The characteristics of the profiles and spectrum remind us of DNOS effect used to explain a slight redshift in the reflection spectrum of long pulse, as shown in Fig.2(f). Due to the similarity between this two cases as shows in Fig.2, we extend the DNOS theory to the regime of extreme nonlinearity. That is, the redshift produced in region I can be explained by the motion of the absorption front near surface instead of FWM.

Several unique features of the few-cycle cases have to be emphasized. Since the few-cycle pulse is more robust against reflection due to the high intensity, it can propagate through the medium with a higher speed instead of penetrating within a nonlinear skin depth as shown in Fig.1 (a) and (b). The velocity of the moving front is close to c, which invalids the image-source method used to derive the equation $\Delta\lambda/\lambda_0 = 2v/c$ used in DNOS [14]. Thus, we use a substituted equation $\nu = \frac{c-v}{c+v}\nu_0$ to obtain the redshift of the reflected pulse due to the Doppler effect for v is close to c [15]. In region I, sample two random times, we get $v_1 = 2.026 \times 10^8\text{m/s}$, $v_2 = 1.61 \times 10^8\text{m/s}$, the corresponding frequencies in reflection spectrum are $\nu_1 = 0.3\nu_0, \nu_2 = 0.53\nu_0$. Compared Fig.1 (a) and (b)
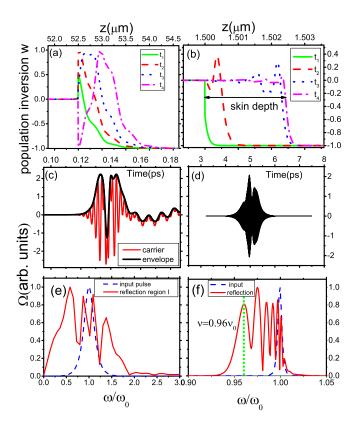
FIG. 2: (color online) The compairation between a few-cycle pulse in region I (a)(c)(e) and a long pulse (b)(d)(f) in terms of population difference (a)(b), reflected field profile (c)(d) and spectrum(e)(f). The parameters for the few-cycle pulse $\tau_p = 5$fs, $A = 4\pi$, $\omega_c = 0.1$fs^{-1}, $\lambda_0 = 830$nm, $t_1 = 83.75$fs (solid line), $t_2 = 85$fs(dashed line), $t_3 = 86.25$fs(dotted line), $t_4 = 87.625$fs(dashed-dotted line); a long pulse $\tau_p = 300$fs, $A \approx 10\pi$, $\omega_c = 6.86$fs^{-1}, $\lambda_0 = 942$nm, $t_1 = 2.16$ps, $t_2 = 2.415$ps, $t_3 = 2.755$ps,$t_4 = 3.095$ps. The skin depth is the location corresponding to t_4. The maximum velocity for (a) and (b) is $v_m = 0.68c$ and $v_m^l = 0.0183c$ respectively. The corresponding redshift is $\nu_m = 0.3\nu_0$ and $\nu_m^l = 0.96\nu_0$, respectively

spectrum II, it can be inferred, in general, the function of region I is adding local oscillations to the original smooth spectrum produced in region II. Moreover, owing to the ultrashort and intense features of the few-cycle pulses, effects such as the carrier Rabi flopping, self-phase modulation and intrapulse FWM may take place, which enrich the spectrum of region I in terms of the appearance of blueshift as shown in Fig.2 (e) and (f).

Now let us move on to the second region, where DNOS effect itself is not sufficient to explain the electric profile. In this region, multiple Rabi flopping causes 4π pulse to split into two 2π pulse [16]. The first one is more intense and propagates much faster than the second one. These two splitted 2π pulses completely excite and deexcite the DTLA medium in different locations, resulting in two moving absorption fronts which travel

with the 2π pulses respectively. The frequencies of the backpropagation waves are obviously velocity-dependent. Those two low-frequency backpropagation waves may interfere with each other, giving rise to the electric profile shows in region II. Note that, the remarkable difference between the region I and region II is the number of effective self-reflected interface and thus the number of the low-frequency components. Specifically, just one interface appears in the former while for the latter it is relied on the area of the input pulse. Also, the first 2π pulse propagates much faster than the 4π pulse penetrating through the interface, such that the self-reflected wave related to the first 2π pulse possess a much larger redshift than that in region I.

At the beginning of the region II around 0.15ps, the absorption fronts are moving forward with a rate $v_1 = 2.66 \times 10^8$m/s and $v_2 = 1.33 \times 10^8$m/s for the first and second pulses, respectively. With the propagation proceeding, the velocity changes of the first 2π pulse is negligible while the second one experiences a deceleration with $a \approx -1.74 \times 10^{20}$m/s^2. For the first pulse, $t = 0.15$ps, $v_1 = 2.66 \times 10^8$m/s, $\nu_1 = 0.06v_0$; $t^{'} = 0.643$ps, $v_1^{'} = 2.74 \times 10^8$m/s, $\nu_1^{'} = 0.045\nu_0$, where t and $t^{'}$ present the moment region II begins and that one of the pulse is outside of the medium, respectively. Note that, redspike I is right centered at $\nu = 0.056\nu_0$ with $\tau = 0.01\nu_0$ as mentioned above. This indicates that the motion of absorbing front induced by the first 2π pulse is responsible for the emergence of the redspike I. By that analogy, for the second 2π pulse $t = 0.15$ps, $v_1 = 1.33 \times 10^8$m/s, $\nu_1 = 0.39v_0$; $t^{'} = 0.643$ps, $v_1^{'} = 0.3 \times 10^8$m/s, $\nu_1^{'} = 0.8v_0$, it's fair to extrapolate that redspike II is related to the propagation of the second 2π pulse and its speed variation is the root of the spectrum broading of this spike.
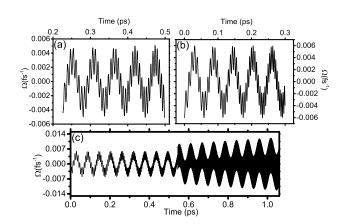
To confirm our theory, we give a interference model

FIG. 3: The comparison of reflected field profiles between numerical result and interference model. (a) is the electric profile during the first several ps in region II, (b) is the counterpart obtained by interference model. (c)is the longer time version of the interference model.

for the backpropation waves. $\Omega(z,t) = \Omega_{01}\cos(\omega_1 t + k_1 z)\hat{e}_z + \Omega_{02}(t)\cos(\omega_2(t)t + k_2 z)\hat{e}_z$, where $v_2(t) = v_{20} - at$, $\omega_2(t) = \frac{c-v_2(t)}{c+v_2(t)}\omega_0$, ω_1 and ω_2 (t) (Ω_{01} and $\Omega_{02}(t)$) are the frequencies (amplitude profiles) of the reflected electric field of first and second 2π pulses, respectively. v_1 and $v_2(t)$ are the speed of the absorbing front propagating along $+z$, $z = 0$ is where detector is placed. Substitute the variables with the following parameters: $v_{20} = 1.3 \times 10^8$m/s, $a = -1.74 \times 10^{20}$m/s^2, $\omega_0 = 2.3$fs^{-1}, Ω_{01}=4×10^{12}Hz. Ω_{02} =2×10^{12}Hz before the first pulse propagates outside the medium and begins to increase due to the influence of the reflection of the first pulse occurred in the back interface. Thus, we obtain the electric profile in Fig.3. Our interference theory is qualitatively in accordance with the numerical results.

In region III, the reflected fields of the first pulse by output interface approach the detector and destroy the profile in region II. Initially, redshift is disappeared in the spectrum due to the immobilized reflector, then the fields are suffered from absorption during the propagation to the detector, leaving a hole in the spectrum at $\omega = \omega_0$. When this reflected fields meet with the back waves produced by the second pulse, the redshift with relatively high frequency is visible in the spectrum, as shown in Fig.1 (b) III.

To sum up, the redshifts are result from the Doppler effect induced by the motion of the self-reflection interface. The previous suggestions that both the redshifts and bluehifts in reflected and transmitted fields are the results of intrapulse FWM is questionable, if not inaccurate. To be more persuasive, we discuss the factors that affect the redshifts and predict the changes of the redshift in spike I with laser and medium parameters

First, we discuss the impact of density by reducing the density. Fig. 4(a) and (b) depict the variation of the transmitted and reflected spectrum with the density is decreased from ω_c =1.0fs^{-1} to ω_c =0.05fs^{-1}. Fig. 4 (c) illustrates the dependence of redshift of spike I on density, which show decrease in a linear pattern. It can be seen, the redspike I in Fig.4 (b) is moving towards the redside with a declining amplitude, while the bulueshift is tend to be diminished as shown in Fig.4 (a). Interestingly, the responses of the redshift and blueshift to the density reduction is quite opposite, which suggests that the physics behind them may not be uniformed. Abandon the idea that both the shift is result from FWM, the observed change rules can be explained very well with the velocity-dependent theory. Specifically, since the red spikes are produced by the propagation of the splitted pulses, lowing density will certainly increase their speed. The motions of the complete population inversion induced by the pulses also speed up. Therefore, the redshift is increased in the consequence of the acceleration of the reflector.

Fig.4(d) reveals the scaling law for laser area. With the increasing of the input pulse area, the frequency of the redspike I experiences a exponential decline. This is because, with a fixed duration τ_p, increasing the area is actually increasing the intensity. The intensity and
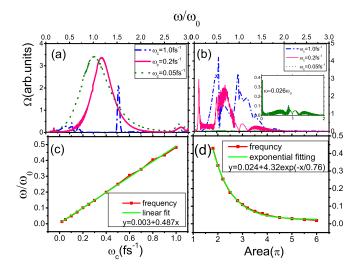

FIG. 4: (color online) The transmitted (a) and reflected (b) spectrums for different density, ω_c =1fs^{-1}(dotted-dashed line), ω_c =0.2fs^{-1}(solid line), ω_c =0.05fs^{-1}(dotted line), with L=150μm, Ω = 1.4fs^{-1}. The inset in (b) is the enlarged view of ω_c =0.05fs^{-1}. (a)-(c) are the changes of amplitude (solid line) and frequency (dashed line) of the redspike I with medium density and pulse area. The other parameters are L=45μm, Ω = 1.4fs^{-1}, ω_c =0.2fs^{-1}, Ω = 1.4fs^{-1}.

duration of the first 2π pulse obtained from Rabi flops is dependent on the intensity of the input pulse. The more intense the input pulse is, the shorter and more intense the first 2π pulse is. As is known, the shorter intense 2π pulse can exchange energy with medium rapidly and thus propagate with a higher speed, which is responsible for a lager redshift.

In conclusion, we give a thorough discussion about the reflected fields of a few-cycle pulse propagation through a DTLA medium and the physics mechanism behind the whole propagation process. The Doppler effect induced by the moving reflector both near and inside the medium are responsible for the redshift in the spectrum. Few-cycle pulses in region I can also have a DNOS alike effect, which results in the interference between input and reflected fields. The reshift produced during this region is relatively small due to the lower speed compared with that in region II. The interference of the two backward propagation waves produces the electric profile observed in the region II. For a 4π pulse, the redshift spike with the largest shift is related to the first 2π pulses, while the second redshift with higher frequencies is related to the second pulse. With the knowledge that the origin of the redspikes appear in the reflected spectrum is related to the doppler shift of backpropagation waves, the redshift can be controlled in terms of its location and amplitude by varying parameters such as medium density and laser intensity to change the reflector. Material structures that are specifically designed to broken the self-reflect inter-

face can also be used to suppress redshift.

---

[1] J. Zhou et al., Opt. Lett. 19, 1149 (1994); A. Stingel et al., Opt. Lett. **20**, 602 (1995).

[2] M. Nisoli et al., Opt. Lett. **22**, 522 (1997).

[3] J. E. Rothenberg, Opt. Lett. **17**, 1340 (1992); Y.P. Niuet al., Phys. Rev. A **78**, 063835 (2008).

[4] R. K. Bullough, P. M. Jack, P. W. Kitchenside and R. Saunders,Phys. Scr. **20**, 364 (1979); J. C. Eilbeck, Gen. Phys. **5**, 1355 (1972); J. C. Eilbeck and R. K. Bullough, Gen. Phys. **5**, 820 (1972).

[5] W.Forysiak, R.G. Flesch, and J.V. Moloney, Phy. Rev. Lett. **76**, 3695 (1996); L. R. F., Phy. Rev. Lett. **55** 2149 (1985); L. R. F., J. Opt. Soc. Am. B **4**, 11 (1987).

[6] R. Marskar and U. L. Österberg, Phys. Rev. A **89**, 023828 (2014).

[7] V.P. Kalosha and J. Herrmann, Phys. Rev. Lett. **83**, 544 (1999).

[8] X. T. Xie and M. A. Macovei, Phys. Rev. Lett **104**, 073902 (2010).

[9] L. Allen and J.H. Eberly, Optical Resonance and Two-Level Atoms (Wiley, New York, 1975); S.L. McCall and E.L. Hahn, Phys. Rev.183, 457 (1969); G.L. Lamb, Jr., Rev. Mod. Phys. **43**,99 (1971).

[10] R.W. Ziolkowski, J.M. Arnold, and D.M. Gogny, Phys. Rev. A **52**, 3082 (1995).

[11] S. Hughes, Phys. Rev. Lett. **81**, 3363 (1998).

[12] K.S. Yee, IEEE Trans. Antennas Propag. **14**, 302 (1996).

[13] A. Taflove and M.E. Brodwin, IEEE Trans. Microwave Theory Tech. **23**, 623 (1975).

[14] A.Sommerfeld,Optics(Academic Press, San Diego,1949), pp.72-75.

[15] The mirror moves away from the source with velocity v, and wave velocity is $u, u > v$. Assume the first wave front is reflected at time t, and the second wave front meets the mirror at $t + \tau$. In this case, $\tau = \frac{\lambda_0}{u-v}$ and the wavelength λ of the reflected light by a moving mirror is the distance between second and first wave front at $t + \tau, \lambda = \frac{u+v}{u-v}\lambda_0, \nu = \frac{u}{\lambda} = \frac{u+v}{u-v}\nu_0$.

[16] J. Xiao, Z. Y. Wang, and Z. Z. Xu, Rhys. Rev. A **63**, 031402 (2002); Chin. Phys. **10**, 0941 (2001).